The PYL4 A194T Mutant Uncovers a Key Role of PYR1-LIKE4/PROTEIN PHOSPHATASE 2CA Interaction for Abscisic Acid Signaling and Plant Drought Resistance[1][C][W][OPEN]

Gaston A. Pizzio, Lesia Rodriguez, Regina Antoni, Miguel Gonzalez-Guzman, Cristina Yunta, Ebe Merilo, Hannes Kollist, Armando Albert, and Pedro L. Rodriguez*

Instituto de Biologia Molecular y Celular de Plantas, Consejo Superior de Investigaciones Cientificas-Universidad Politecnica de Valencia, ES–46022 Valencia, Spain (G.A.P., L.R., R.A., M.G.-G., P.L.R.); Departamento de Cristalografía y Biología Estructural, Instituto de Química Física Rocasolano, Consejo Superior de Investigaciones Científicas, ES–28006 Madrid, Spain (C.Y., A.A.); and Institute of Technology, University of Tartu, Tartu 50411, Estonia (E.M., H.K.)

Because abscisic acid (ABA) is recognized as the critical hormonal regulator of plant stress physiology, elucidating its signaling pathway has raised promise for application in agriculture, for instance through genetic engineering of ABA receptors. PYRABACTIN RESISTANCE1/PYR1-LIKE (PYL)/REGULATORY COMPONENTS OF ABA RECEPTORS ABA receptors interact with high affinity and inhibit clade A phosphatases type-2C (PP2Cs) in an ABA-dependent manner. We generated an allele library composed of 10,000 mutant clones of Arabidopsis (*Arabidopsis thaliana*) PYL4 and selected mutations that promoted ABA-independent interaction with PP2CA/ABA-HYPERSENSITIVE3. In vitro protein-protein interaction assays and size exclusion chromatography confirmed that PYL4^{A194T} was able to form stable complexes with PP2CA in the absence of ABA, in contrast to PYL4. This interaction did not lead to significant inhibition of PP2CA in the absence of ABA; however, it improved ABA-dependent inhibition of PP2CA. As a result, 35S:PYL4^{A194T} plants showed enhanced sensitivity to ABA-mediated inhibition of germination and seedling establishment compared with 35S:PYL4 plants. Additionally, at basal endogenous ABA levels, whole-rosette gas exchange measurements revealed reduced stomatal conductance and enhanced water use efficiency compared with nontransformed or 35S:PYL4 plants and partial up-regulation of two ABA-responsive genes. Finally, 35S:PYL4^{A194T} plants showed enhanced drought and dehydration resistance compared with nontransformed or 35S:PYL4 plants. Thus, we describe a novel approach to enhance plant drought resistance through allele library generation and engineering of a PYL4 mutation that enhances interaction with PP2CA.

Abscisic acid (ABA) plays a critical role both for plant biotic and abiotic stress response (Cutler et al., 2010). Because ABA is recognized as the critical hormonal regulator of plant response to water stress, both the ABA biosynthetic and signaling pathways can be considered as potential targets to improve plant performance under drought. Thus, it has been demonstrated that transgenic plants producing high levels of ABA display improved growth under drought stress compared with the wild type (Iuchi et al., 2001; Qin and Zeevaart, 2002). Priming of ABA biosynthesis can be obtained by direct overexpression of 9-cis-epoxycarotenoid dioxygenase, a key enzyme in the biosynthetic pathway (Iuchi et al., 2001; Qin and Zeevaart, 2002), or through the use of chemicals that accelerate ABA accumulation (Jakab et al., 2005). On the other hand, some examples are also known of Arabidopsis (*Arabidopsis thaliana*) mutants affected in ABA signaling that show both an enhanced ABA response and drought-resistant phenotypes (Pei et al., 1998; Hugouvieux et al., 2001; Saez et al., 2006). For instance, enhancement of ABA sensitivity and reduction of water consumption has been achieved in Arabidopsis by combined inactivation of the protein phosphatases type 2C (PP2Cs) ABA-INSENSITIVE1 (ABI1) and HYPERSENSITIVE TO ABA1 (HAB1), leading to drought-resistant plants (Saez et al., 2006). Enhancing ABA signaling through the recently discovered PYRABACTIN RESISTANCE (PYR)/PYR1-LIKE (PYL)/REGULATORY COMPONENTS OF ABA RECEPTORS (RCAR) ABA receptors is another promising approach to improve plant drought resistance,

[1] This work was supported by the Ministerio de Ciencia e Innovacion, Fondo Europeo de Desarrollo Regional, and Consejo Superior de Investigaciones Cientificas (grant nos. BIO2011–23446 to P.L.R and BFU2011–25384 to A.A., fellowships to R.A. and L.R., and a Juan de la Cierva contract to M.G.-G.) and the Estonian Ministry of Science and Education and European Regional Fund (IUT2–21 and Center of Excellence Environ to E.M. and H.K.).

* Address correspondence to prodriguez@ibmcp.upv.es.

The author responsible for distribution of materials integral to the findings presented in this article in accordance with the policy described in the Instructions for Authors (www.plantphysiol.org) is: Pedro L. Rodriguez (prodriguez@ibmcp.upv.es).

[C] Some figures in this article are displayed in color online but in black and white in the print edition.

[W] The online version of this article contains Web-only data.

[OPEN] Articles can be viewed online without a subscription.

www.plantphysiol.org/cgi/doi/10.1104/pp.113.224162

for instance through overexpression or generation of constitutively active (CA) receptors (Santiago et al., 2009b; Saavedra et al., 2010; Mosquna et al., 2011). However, pleiotropic effects due to sustained effects of high ABA levels or active ABA signaling might negatively affect plant growth, because abiotic stress responses divert resources required for normal growth. For instance, it was shown that vegetative expression of CA receptors was posttranscriptionally abolished in the case of PYL2 (Mosquna et al., 2011).

Recent studies reveal at least two subclasses of PYR/PYL receptors, including monomeric and dimeric PYLs (Dupeux et al., 2011a; Hao et al., 2011). The dimeric receptors (PYR1, PYL1, and PYL2) show a higher dissociation constant for ABA (>50 μM, lower affinity) than monomeric ones (approximately 1 μM); however, in the presence of certain clade A PP2Cs, both groups of receptors form ternary complexes with high affinity for ABA (dissociation constant, 30–60 nM; Ma et al., 2009; Santiago et al., 2009a, 2009b). A third subclass appears when we consider the transdimeric PYL3 receptor, which suffers a cis- to trans-dimer transition upon ligand binding to facilitate the subsequent dissociation to monomer (Zhang et al., 2012). Dimeric receptors occlude their surface of interaction with the PP2C in the dimer, so they are strongly ABA dependent for dissociation and adoption of a PP2C-binding conformation (Dupeux et al., 2011a). In vitro, monomeric ABA receptors are able to interact in the absence of ABA to some extent with the catalytic core of ABI1/ABI2/HAB1/PP2CA phosphatases, although less stable complexes are formed compared with ternary complexes with ABA (Dupeux et al., 2011a; Hao et al., 2011; Antoni et al., 2013). Boosting of such interaction might lead to faster association kinetics with PP2Cs or faster response to low-intermediate ABA levels. A subbranch of clade A PP2Cs comprises Highly ABA-Induced (HAI) phosphatases that show a more restrictive pattern of interaction with PYR/PYLs compared with ABI1/ABI2/HAB1/PP2CA (Bhaskara et al., 2012).

Yeast (*Saccharomyces cerevisiae*) two-hybrid (Y2H) assays reveal both ABA-independent and -dependent interactions among PYR/PYLs and PP2Cs (Ma et al., 2009; Park et al., 2009; Santiago et al., 2009b). However, tandem affinity purification of PYL8-interacting partners in planta was largely dependent on ABA to recover PYL8-PP2C complexes (Antoni et al., 2013). Y2H interactions of PYR/PYLs and PP2Cs that are dependent on exogenous ABA offer the possibility to set up screenings involving the generation of allele libraries and growth tests aimed to identify mutations that render ABA-independent interactions. Such mutations might lead in the plant cell to receptors that (1) show enhanced association kinetics with PP2Cs by generating additional contact points and (2) interfere with PP2C function by steric hindrance or, when several mutations are combined, to CA receptors that inhibit PP2Cs in the absence of ABA. The interaction in Y2H assays of PYL4 and PP2CA, two representative members of the PYR/PYL and clade A PP2C families, respectively, was shown to be ABA dependent (Lackman et al., 2011). PYL4 shows high expression levels in different tissues, and its inactivation is required to generate strongly ABA-insensitive combined *pyr/pyl* mutants (Gonzalez-Guzman et al., 2012). PP2CA plays a critical role to regulate both seed and vegetative responses to ABA and regulates stomatal aperture through interaction with the anion channel SLOW ANION CHANNEL1 (SLAC1) and the kinase OPEN STOMATA1 (OST1; Kuhn et al., 2006; Yoshida et al., 2006; Lee et al., 2009). Therefore, PP2CA is a physiologically relevant target to design PYR/PYL receptors that show enhanced interaction with the phosphatase, affecting ABA signaling and plant stress response.

Through the generation of a PYL4 allele library and Y2H assays, we selected several PYL4 mutations enabling ABA-independent interaction with PP2CA in yeast. We focused our work on the PYL4^{A194T} protein, which interacted with PP2CA in the absence of ABA. This interaction led to a very modest inhibition of PP2CA in the absence of ABA (using *p*-nitrophenyl phosphate [pNPP] as a phosphatase substrate); however, it improved ABA-dependent inhibition of PP2CA. As a result, upon overexpression of PYL4^{A194T}, we observed enhanced sensitivity to ABA compared with nontransformed or 35S:PYL4 plants both in seed and vegetative tissues. Moreover, 35S:PYL4^{A194T} transgenic plants showed enhanced drought resistance compared with nontransformed or 35S:PYL4 plants. By contrast, a previous attempt to express a mutagenized version of an ABA receptor failed to detect protein expression in vegetative tissue, and therefore phenotype analysis could only be performed in seeds (Mosquna et al., 2011).

RESULTS

Identification of PYL4 Mutations That Promote ABA-Independent Interaction with PP2CA in Yeast

PYL4 interacts in an ABA-dependent manner with PP2CA in Y2H assays (Lackman et al., 2011; Fig. 1A). We conducted error-prone PCR mutagenesis of the PYL4 receptor and generated an allele library of approximately 10,000 clones in the pGBKT7 vector. The library was shuttled to yeast AH109 by cotransformation with pGAD7-PP2CA. Yeast transformants were pooled, and clones able to grow in the absence of exogenous ABA in medium lacking His and adenine were selected. Yeast plasmids were extracted, sequenced, and retransformed in yeast cells to recapitulate the phenotype. Thus, different mutations in the encoded PYL4 protein were identified that enabled constitutive interaction with PP2CA (Fig. 1, A and B). Through site saturation mutagenesis of PYR1, Mosquna et al. (2011) identified mutations located in 10 different residues of the receptor that promoted PYR1-HAB1 interactions in the absence of ABA. These mutations were clustered in the receptor-phosphatase interaction surface, specifically in the gating loop of PYR1, its C-terminal α-helix, and H60. The H60 of PYR1 is a hotspot for activating mutations, and for instance, the H60P substitution destabilizes the PYR1

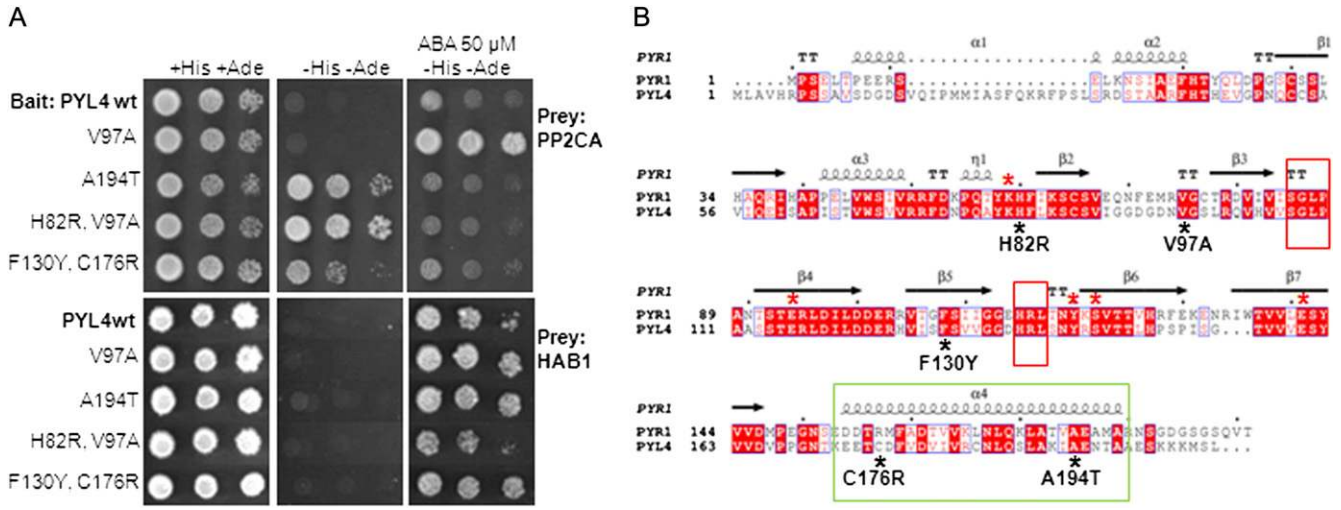

Figure 1. Identification of PYL4 mutations that generate ABA-independent interaction with PP2CA in a Y2H assay. A, Interaction of PYL4 or PYL4 mutants (baits, fused to the Gal4 binding domain) and either PP2CA or HAB1 (preys, fused to the Gal4 activating domain). Interaction was determined by growth assay on medium lacking His and Adenine. When indicated, the medium was supplemented with 50 μM ABA. Dilutions (10^{-1}, 10^{-2}, and 10^{-3}) of saturated cultures were spotted onto the plates, and photographs were taken after 7 d. B, Alignment of PYR1 and PYL4 amino acid sequences and secondary structure. Location of the PYL4 mutations is marked by black asterisks. Red boxes indicate the position of the gate and latch loops. The green box indicates the position of the C-terminal α-helix. Red asterisks mark K59, E94, Y120, S122, and E141 residues of PYR1 involved in ABA binding. [See online article for color version of this figure.]

dimer and increases its apparent ABA affinity and both PYR1^{H60P} and PYR1^{H60R} bound HAB1 in the absence of ABA (Dupeux et al., 2011a; Mosquna et al., 2011). The H60 equivalent residue in PYL4 is H82, and interestingly we found in our screening a PYL4^{H82R} mutation that resulted in ABA-independent interaction with PP2CA (Fig. 1A). The H82R mutation was found combined with V97A but the individual V97A mutation did not affect the interaction in the absence of ABA, although it increased yeast growth in the presence of ABA (Fig. 1A). Other mutations that enhanced the interaction of PYL4 and PP2CA in the absence of ABA were A194T and the double mutation F130Y C176R (Fig. 1, A and B). Both A194T and C176R mutations are located in the C-terminal helix of PYL4, which represented another hotspot for activating mutations in PYR1 because this α-helix forms part of the receptor-phosphatase binding interface (Mosquna et al., 2011). The interaction of the PP2C HAB1 with PYL4 was also found to be ABA dependent in yeast (Lackman et al., 2011), so we decided to test whether the PYL4-described mutations affected the interaction with HAB1 in the absence of ABA. However, in contrast to their effect on the interaction with PP2CA, these mutant versions of PYL4 behaved mostly as PYL4 when assayed with HAB1 (Fig. 1A).

Effect of PYL4 Mutations on PP2CA Activity in Vitro

Y2H assays reveal both ABA-independent and -dependent interactions among PYR/PYLs and PP2Cs; however, PYR/PYL receptors inhibit the activity of clade A PP2Cs mostly in an ABA-dependent manner (Fujii et al., 2009; Ma et al., 2009; Park et al., 2009; Santiago et al., 2009b). Thus, an ABA-independent interaction in Y2H assay does not necessarily imply capacity to inhibit phosphatase activity in the absence of ABA. Although most of the monomeric PYR/PYL receptors show ABA-independent interaction with different PP2Cs in Y2H assay, effective phosphatase inhibition requires ABA, and for instance, the in vivo binding of PYL8 to five clade A PP2Cs was largely dependent on ABA (Ma et al., 2009; Park et al., 2009; Santiago et al., 2009b; Antoni et al., 2013). Therefore, we tested whether these mutations affected actually the activity of two clade A PP2Cs, i.e. PP2CA and HAB1. Using pNPP as a substrate, we could detect a small inhibitory effect (20%) of PYL4^{A194T} on the activity of PP2CA in the absence of ABA with respect to PYL4 (Fig. 2A). However, although the H82RV97A and F130Y C176R mutations promoted ABA-independent interactions in Y2H assay, they did not affect PP2CA activity in the absence of ABA. In the presence of 1 μM ABA, PYL4^{A194T} also showed a higher inhibition of PP2CA than PYL4 (Fig. 2A). The other mutations behaved similarly to PYL4 except F130Y C176R, which showed lower capacity to inhibit PP2CA in the presence of ABA. PYL4 inhibited more efficiently HAB1 than PP2CA (inhibitory concentration to obtain 50% inhibition of 0.25 and 1 μM, respectively), and all PYL4 mutants inhibited HAB1 similarly to PYL4 (Fig. 2B).

Although phosphatase activity is usually measured using small phosphorylated molecules such as pNPP or phosphopeptides, in vivo phosphatase activity is addressed against phosphorylated proteins and therefore could involve substrate-dependent effects. Therefore, we also performed in vitro reconstitution of the

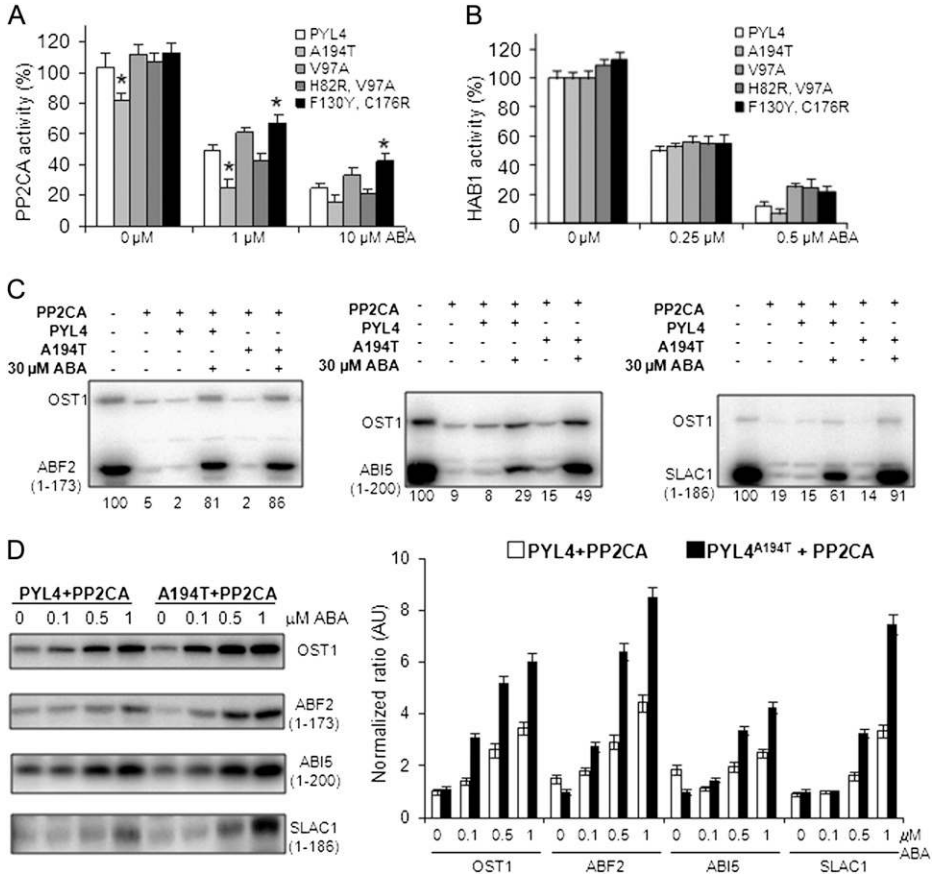

Figure 2. PYL4^{A194T} prevents better than PYL4 the PP2CA-mediated dephosphorylation of protein substrates in the presence of ABA. A and B, Phosphatase activity of either PP2CA or HAB1, respectively, was measured in vitro using pNPP as a substrate in the absence or presence of PYL4 or different PYL4 mutant versions at the indicated ABA concentrations. Assays were performed in a 100-μ reaction volume that contained 2 μM phosphatase and 4 μM receptor. Data are averages ± SE from three independent experiments. Asterisk indicates $P < 0.05$ (Student's t test) when comparing data of mutant and wild-type PYL4 in the same assay conditions. C and D, Effect of PYL4^{A194T} or PYL4 on PP2CA-mediated dephosphorylation of OST1, ABF2 (1–173), ABI5 (1–200), and SLAC1 (1–186) phosphorylated proteins. C, The quantification of the autoradiography (numbers below) shows the percentage of protected phosphorylated substrate in each experiment relative to 100% in the absence of PP2CA. A 1:10 phosphatase:receptor stoichiometry was used in this assay. D, PYL4^{A194T} prevents better than PYL4 the PP2CA-mediated dephosphorylation of OST1, ABF2 (1–173), ABI5 (1–200), and SLAC1 (1–186). Value 1 expresses protection of each substrate in the absence of ABA, and the normalized ratio expresses the fold number that either PYL4^{A194T} or PYL4 enhanced protection of the substrate at the indicated concentration of ABA. A 1:1 phosphatase:receptor stoichiometry was used in this assay.

ABA signaling cascade and measured the capacity of PYL4^{A194T} or PYL4 to inhibit the dephosphorylation of several PP2CA targets, i.e. OST1/SnRK2.6, C-terminal deletion (ΔC)-ABRE binding factor2 (ABF2; residues 1–173), and ΔC-ABA-INSENSITIVE5 (ABI5; residues 1–200) transcription factors or N-terminal fragment (residues 1–186) of the anion channel SLAC1 (Fig. 2C). First, a phosphorylation reaction was performed where OST1 was autophosphorylated in vitro, and, in turn, it phosphorylated ΔC-ABF2, ΔC-ABI5, and SLAC1$^{1–186}$ proteins. Next, these proteins were used as substrates of PP2CA that was preincubated (or not) for 10 min with PYL4 or PYL4^{A194T} either in the absence or presence of 30 μM ABA. In the absence of ABA, we did not find significant differences among PYL4 and PYL4^{A194T}. In the presence of 30 μM ABA, PYL4^{A194T} inhibited better than PYL4 the dephosphorylation by PP2CA of ΔC-ABI5 and SLAC1$^{1–186}$, although it was not more effective than PYL4 to inhibit the dephosphorylation of ΔC-ABF2 (Fig. 2C). PYL4^{A194T} shows enhanced capacity to interact with PP2CA in the absence of ABA, probably because novel contact points are generated by the mutation. Therefore, we reasoned that this mutation might also lead to enhanced association kinetics in the presence of ABA, particularly at low ABA levels or low phosphatase:receptor ratios. We performed dephosphorylation assays at low ABA concentrations (0.1, 0.5, and 1 μM) and 1:1 phosphatase:receptor ratio (Fig. 2D). In the presence of 0.5 to 1 μM ABA, PYL4^{A194T} inhibited better (2–3-fold) than PYL4 the dephosphorylation of ΔC-ABF2, ΔC-ABI5, and SLAC1$^{1–186}$. Protection of OST1 phosphorylation

was also improved by PYL4^{A194T} compared with PYL4 (Fig. 2D).

In Vitro and in Vivo Interaction of PYL4^{A194T} and PP2CA

The phenotype described below for 35S: PYL4^{A194T} plants prompted us to further analyze the interaction between PYL4^{A194T} and PP2CA using in vivo and in vitro protein-protein interaction tests. First, bimolecular fluorescent complementation (BiFC) assays were used to analyze the interaction of PYL4 or PYL4^{A194T} and either PP2CA or HAB1 in tobacco (*Nicotiana tabacum*) cells (Fig. 3A). To this end, we performed transient expression of PP2CA-Yellow fluorescent protein N-terminal fragment (YFP^{N}) and Yellow fluorescent protein C-terminal fragment (YFP^{C})-PYL4 in epidermal cells of *Nicotiana benthamiana* using agroinfiltration. The nuclear interaction between PP2CA and PYL4 did not require the addition of exogenous ABA; endogenous ABA levels in tobacco cells after agroinfiltration appear to be enough to promote such interaction. The subcellular localization of PP2CA was previously investigated by Antoni et al. (2012) using both transient expression of PP2CA-GFP in tobacco cells and biochemical fractionation of Arabidopsis transgenic lines that express hemmaglutinin (HA)-tagged PP2CA. We found that PP2CA was localized both to nucleus and cytosol; however, PP2CA-GFP appears to be predominantly localized in the nucleus, and presumably a higher concentration of the protein is found in this compartment (Fig. 3A). Both red fluorescent protein (RFP)-PYL4 and RFP-A194T show a similar localization pattern to each other (Fig. 3A). Injection of ABA enhanced the relative fluorescence of the PP2CA-PYL4 complex and made evident additional interaction at the cytosol (Supplemental Fig. S1). PYL4^{A194T} was able to interact with PP2CA in the cytosol at endogenous ABA levels, and the relative fluorescence emission was higher in the PYL4^{A194T}-PP2CA interaction compared with PYL4 (Fig. 3B). Therefore, our results suggest that A194T is able to interact in the cytosol with PP2CA at low ABA levels, whereas PYL4 is not. In the nucleus, the higher concentration of PP2CA-GFP probably facilitates the BiFC interaction. By contrast, the interaction of HAB1 and either PYL4 or PYL4^{A194T} did not differ significantly (Fig. 3, A and B).

Finally, we performed in vitro protein-protein interaction assays. Non-His-tagged PYL4^{A194T} could be copurified with 6His-ΔNPP2CA using Ni affinity chromatography in the absence of ABA, in contrast to PYL4 (Fig. 3C). Size exclusion chromatography and SDS-PAGE analysis of the eluted fractions confirmed that both proteins formed a 1:1 complex in the absence of ABA (Fig. 3D). Finally, a pull-down assay showed that whereas the interaction of PYL4 and PP2CA was dependent on the addition of ABA, ABA-independent binding could be observed for PYL4^{A194T} and PP2CA (Fig. 3E). Therefore, both in vivo and in vitro assays show a differential interaction of PYL4^{A194T} and PP2CA with respect to PYL4.

Analysis of Transgenic Lines Overexpressing PYL4 Mutants

To study the putative effect of PYL4 mutations on ABA signaling in vivo, we generated transgenic plants that overexpressed HA-tagged versions of PYL4 or the mutant versions PYL4^{V97A}, PYL4^{A194T}, PYL4$^{C176R\ F130Y}$, and PYL4$^{H82R\ V97A}$. Expression of the proteins in vegetative tissue was detected by immunoblot analysis and transgenic lines that expressed similar levels of PYL4, and mutant PYL4 proteins were selected for further analysis; however, PYL4$^{H82R\ V97A}$ lines consistently showed lower expression of the transgene compared with PYL4 or other mutant proteins (Fig. 4A). Overexpression of PYL4 or PYL4^{V97A} enhanced ABA-mediated inhibition of seedling establishment compared with nontransformed plants, whereas ABA sensitivity of PYL4$^{C176R\ F130Y}$ overexpressing (OE) plants was similar to nontransformed plants. Interestingly, both PYL4^{A194T} and PYL4^{H82RV97A} OE plants showed higher sensitivity to ABA-mediated inhibition of seedling establishment than PYL4 OE plants (Fig. 4B). Low concentrations of ABA (0.25–0.5 μM) delay seedling establishment of the nontransformed ecotype Columbia (Col-0) wild type and have a limited inhibitory effect on further growth of the seedlings (Fig. 4C). This effect was enhanced in PYL4 or PYL4^{V97A} OE plants, particularly evident at 0.5 μM ABA (Fig. 4C). In the case of PYL4^{A194T} and PYL4^{H82RV97A} OE plants, the effect was even visible at 0.25 μM ABA, indicating that these lines show higher sensitivity to ABA-mediated inhibition of shoot growth than PYL4 OE plants (Fig. 4, C and D).

Subsequent generations of PYL4^{H82RV97A} transgenic plants showed reduced levels of the protein compared with homozygous T3, so we concentrated further analysis on PYL4^{A194T} transgenic lines, where expression of the transgene remained stable. Seed germination and seedling establishment analyses of PYL4^{A194T} OE lines confirmed the enhanced sensitivity to ABA observed in T3 seeds (Supplemental Fig. S2). Moreover, root and shoot growth analyses also revealed enhanced sensitivity to ABA in vegetative tissues (Fig. 5). We transferred 4-d-old seedlings to Murashige and Skoog (MS) medium plates lacking or supplemented with 10 μM ABA, and root growth was measured 10 d after transfer. Both PYL4 and PYL4^{A194T} OE plants showed enhanced ABA-mediated inhibition of root growth compared with nontransformed plants (Fig. 5, A and B). Shoot growth was evaluated by measuring the maximum rosette radius of plants grown for 11 d in MS medium lacking or supplemented with 10 μM ABA (Fig. 5C). Finally, we measured expression of two ABA-responsive genes, *ABA-responsive18* (*RAB18*) and *desiccation-responsive29B* (*RD29B*), in mock- or 10 μM ABA-treated plants (Fig. 5D). In the absence of exogenous ABA treatment, expression of *RAB18* and *RD29B* was 6- and 23-fold, respectively, up-regulated in PYL4^{A194T} OE plants compared with nontransformed plants. These results indicate a partial derepression of ABA-responsive genes in this line compared with nontransformed plants.

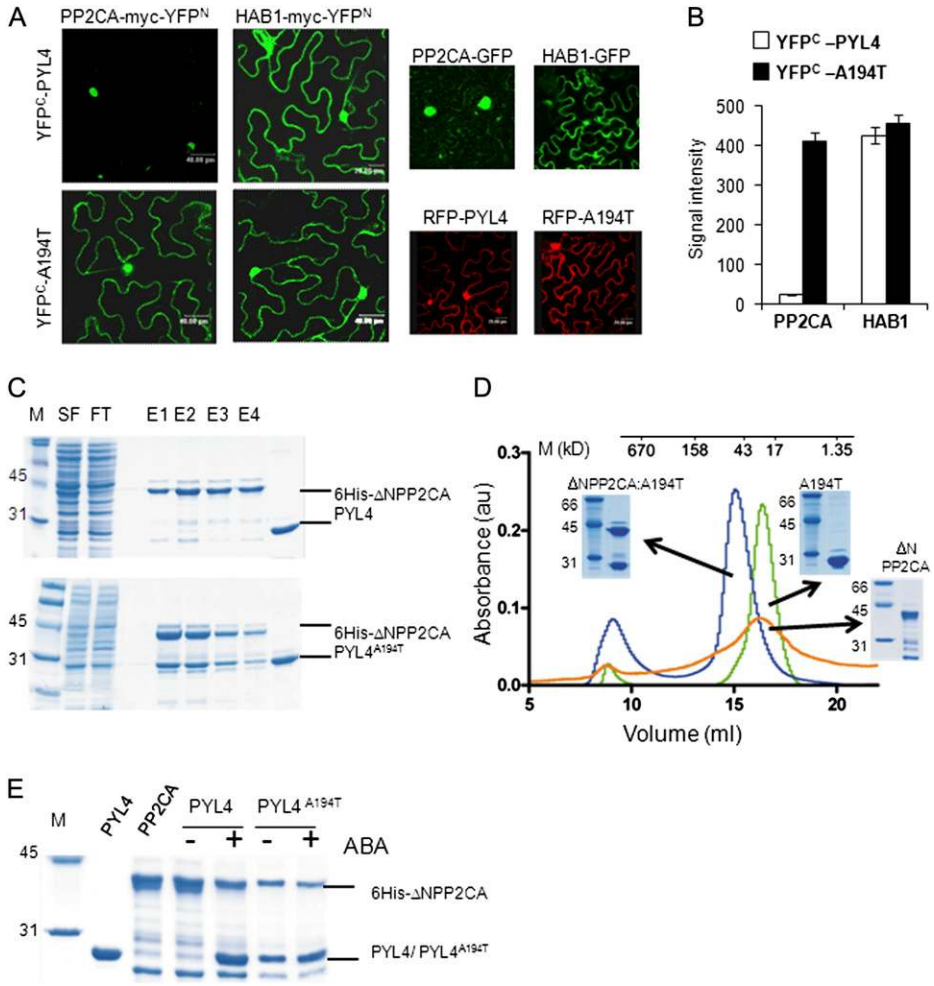

Figure 3. BiFC assay shows a different interaction of PYL4 or PYL4^{A194T} and PP2CA in tobacco leaves. PYL4^{A194T} binds ΔNPP2CA in the absence of ABA in vitro. A, Laser scanning confocal imaging of epidermal leaf cells infiltrated with a mixture of *A. tumefaciens* suspensions harboring the indicated BiFC constructs and the silencing suppressor p19. Right panels show the location of GFP and RFP fusions of PP2Cs and receptors, respectively. B, Quantification of the fluorescent protein signal. Images of A were analyzed using ImageJ software, and signal intensity was calculated after subtracting the mean background density. C, SDS-PAGE showing the Ni^{2+} affinity chromatography purification from *E Escherichia coli* lysates containing recombinant 6His-ΔNPP2CA and either PYL4 (top) or PYL4^{A194T} (bottom). A lane showing PYL4 and PYL4^{A194T} is also displayed at the right of each gel. In the absence of ABA, PYL4^{A194T} copurifies with 6His-ΔNPP2CA, while PYL4 does not. D, Elution profiles after size exclusion chromatography in absence of ABA of pure PYL4^{A194T} (green) and 6His-ΔNPP2CA (orange) and the eluted fractions described above containing the copurified PYL4^{A194T}/6His-ΔNPP2CA (blue) proteins. Insets from each peak show SDS-PAGE analysis. The figure shows the formation of 1:1 PYL4^{A194T}:6His-ΔNPP2CA complex and the monomeric nature of PYL4^{A194T}. E, SDS-PAGE shows a pull-down assay, where 6His-ΔNPP2CA is incubated with PYL4 or PYL4^{A194T} in absence or presence of 100 μM ABA. M, Molecular mass markers; SF, soluble fraction; FT, flow through the column; E1 to E4, eluted fractions at 500 mM imidazole. [See online article for color version of this figure.]

However, after ABA treatment, the induction of these genes was not higher than in nontransformed plants.

PYL4^{A194T} OE Plants Show Enhanced Water Use Efficiency and Drought Resistance

Regulation of stomatal aperture by ABA is a key adaptive response to cope with drought stress. To probe stomatal function in nontransformed Col-0, PYL4, and PYL4^{A194T} OE plants, we performed diurnal analysis of stomatal conductance (Gst) and transpiration in whole plants under basal conditions (Fig. 6, A and B). Interestingly, both PYL4 and PYL4^{A194T} OE lines showed lower Gst and transpiration values than nontransformed Col-0 plants during the day and night. Moreover, PYL4^{A194T} OE plants showed lower Gst values than PYL4 OE plants. Diurnal course of Gst was generally not affected in transformed plants; both OE lines closed their stomata like the nontransformed Col-0 wild type during the night and showed maximum Gst values around midday, followed by predark stomatal closure. Still, predawn stomatal opening was more pronounced

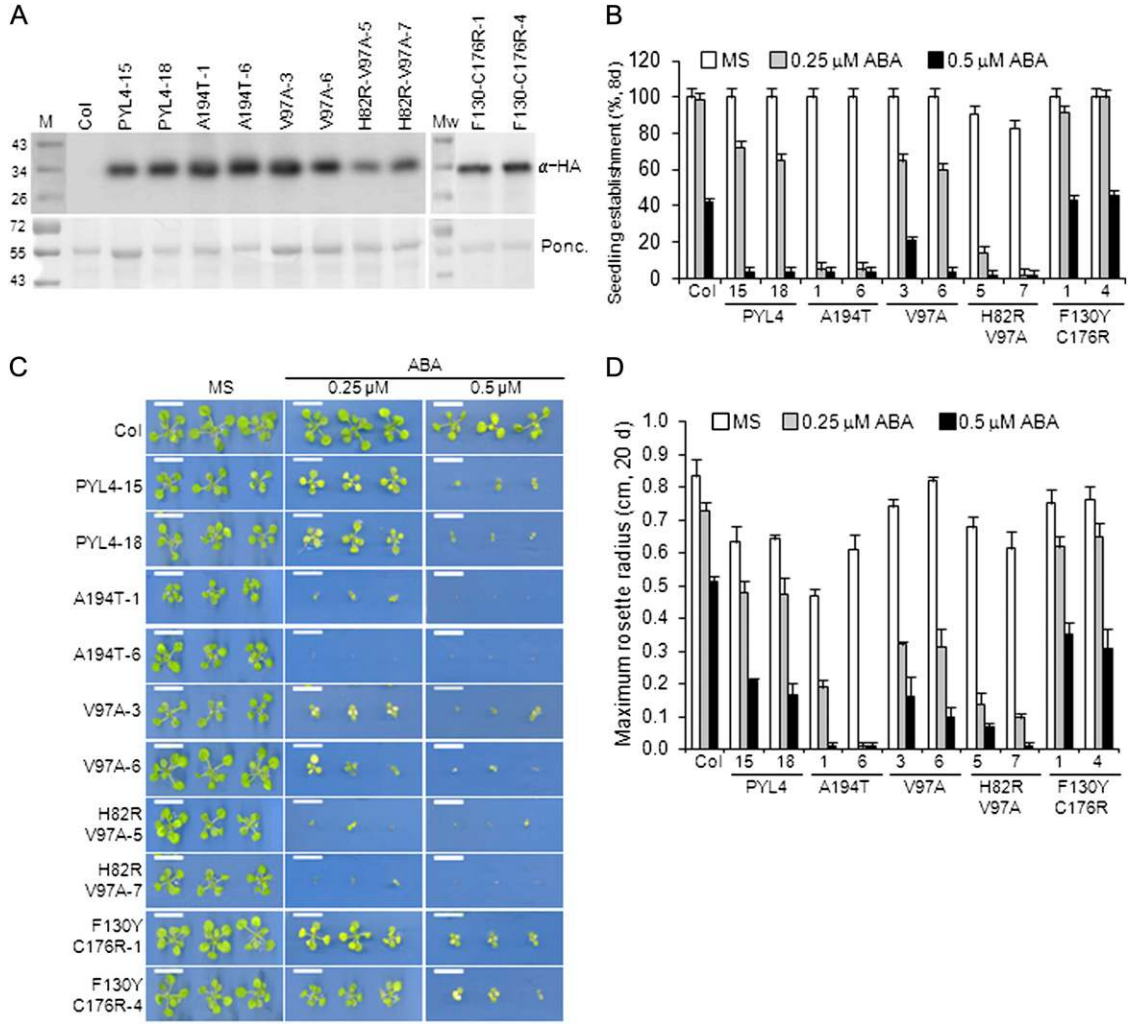

Figure 4. Enhanced sensitivity to ABA-mediated inhibition of seedling establishment and early seedling growth in PYL4 and PYL4^{A194T} OE lines compared with nontransformed Col-0 plants. A, Immunoblot analysis using antibody against HA tag to quantify expression of PYL4, PYL4^{V97A}, PYL4^{A194T}, PYL4$^{C176R\,F130Y}$, and PYL4$^{H82R\,V97A}$ in 21-d-old seedlings of T3 transgenic lines (top). Ponceau staining is shown below. B and C, ABA-mediated inhibition of seedling establishment and early seedling growth in PYL4 and different PYL4^{mutant} OE lines compared with nontransformed Col-0 plants. B, Approximately 100 seeds of each genotype (three independent experiments) were sown on MS plates lacking or supplemented with 0.25 or 0.5 μM ABA. Seedlings were scored for the presence of both green cotyledons and the first pair of true leaves after 8 d. Values are averages ± SE. C, Photographs of representative seedlings were taken 20 d after sowing. D, Quantification of ABA-mediated early seedling growth inhibition in PYL4 and different PYL4^{mutant} OE lines compared with nontransformed Col-0 plants. Data were obtained by measuring maximum rosette radius after 20 d and are averages ± SE from three independent experiments. [See online article for color version of this figure.]

in the nontransformed Col-0 wild type and PYL4 OE compared with PYL4^{A194T} OE plants. The latter result could be directly related to an enhanced ABA sensitivity of PYL4^{A194T} OE plants, because diurnal stomatal movements are linked to ABA concentration via its effect on ion and sugar fluxes (Tallman, 2004).

The lower Gst values of PYL4 and PYL4^{A194T} OE plants suggest that under steady-state conditions, the stomata of PYL4 and PYL4^{A194T} OE plants have reduced aperture compared with nontransformed Col-0 plants. Direct measurements of stomatal aperture using whole-leaf imaging revealed that stomata of both PYL4 and particularly PYL4^{A194T} OE plants were more closed than those of nontransformed Col-0 plants (Fig. 6C). Finally, we also performed water loss assays of nontransformed Col-0, PYL4, and PYL4^{A194T} OE lines (Fig. 6D). Water loss experiments were done using 15-d-old seedlings grown in a growth chamber, which were excised from petri dishes and submitted to the drying atmosphere of a laminar flow hood (Fig. 6D). Water loss kinetics indicated that PYL4^{A194T} OE lines lost less water than nontransformed or PYL4 OE lines (Fig. 6D). Finally, when scoring stomatal aperture, we noticed that stomatal density of PYL4 and PYL4^{A194T} OE lines was

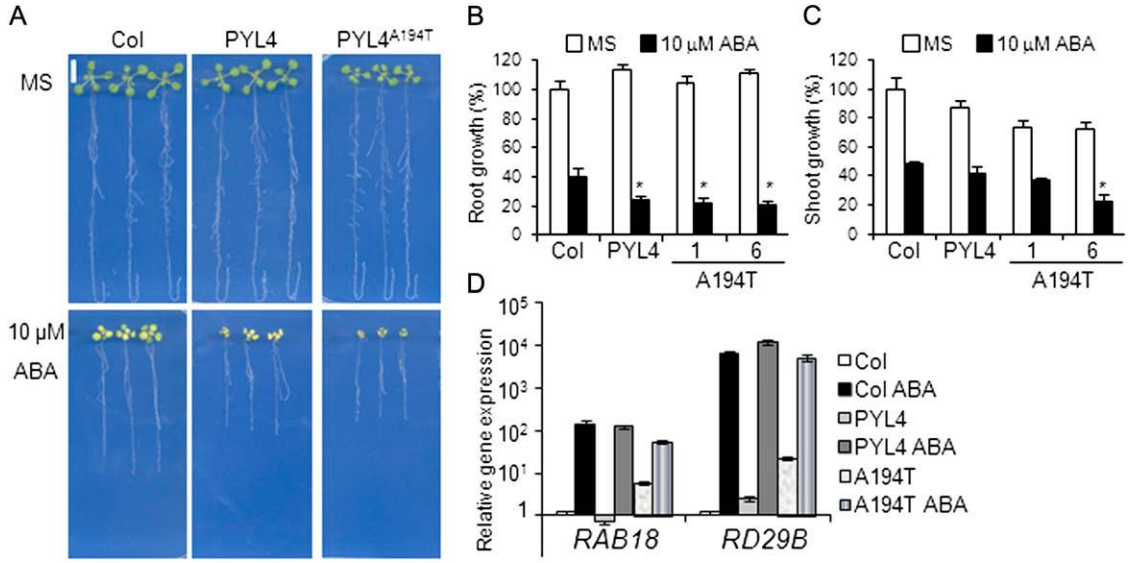

Figure 5. Enhanced sensitivity to ABA-mediated inhibition of root growth of PYL4 and PYL4^{A194T} OE lines compared with nontransformed Col-0 plants. A, Photographs of representative seedlings 10 d after the transfer of 4-d-old seedlings to MS plates lacking or supplemented with 10 μM ABA. B and C, Quantification of ABA-mediated root or shoot growth inhibition, respectively (values are means ± SE; growth of the Col-0 wild type on MS medium was taken as 100%). Asterisk indicates $P < 0.05$ (Student's *t* test) when comparing data of PYL4 or PYL4^{A194T} OE plants with nontransformed Col-0 plants in the same assay conditions. D, PYL4^{A194T} OE plants show partial constitutive up-regulation of ABA-responsive genes in the absence of exogenous ABA. Expression of two ABA-inducible genes, *RAB18* and *RD29B*, in Col-0, PYL4, and PYL4^{A194T} OE plants was analyzed by quantitative reverse transcription-PCR in RNA samples of 2-week-old seedlings that were either mock or 10 μM ABA treated for 3 h. Data indicate the expression level (values are means ± SE) of the *RAB18* and *RD29B* genes in each column with respect to mock-treated Col-0 (value 1). [See online article for color version of this figure.]

circa 10% lower than that of nontransformed plants (Fig. 6E). Therefore, a partial explanation of the reduced water loss observed in these lines can be attributed to 10% reduced stomatal density. However, because stomatal density was similar in PYL4 and PYL4^{A194T} OE lines, but lower transpiration was found in PYL4^{A194T} compared with PYL4 OE lines, we conclude that A194T has a higher effect compared with PYL4.

Reduced net photosynthesis (Anet) could be a drawback caused by the reduced stomatal opening and Gst found in PYL4 and PYL4^{A194T} OE lines. Therefore, to evaluate the performance of these plants compared with nontransformed plants, we determined water use efficiency (WUE), i.e. the amount of carbon gained per unit water lost, Anet/transpiration. Both PYL4 and PYL4^{A194T} OE lines showed a reduced Anet compared with nontransformed plants; however, PYL4^{A194T} OE lines showed enhanced WUE compared with nontransformed and PYL4 OE plants because the strongly reduced transpiration compensated the effect on Anet (Fig. 6F).

Finally, we performed drought resistance experiments under greenhouse conditions (Fig. 7). Plants were grown in a greenhouse under normal watering conditions for 15 d, and then irrigation was stopped. This day was taken as 0 d, when average rosette radius did not differ significantly among nontransformed Col-0, PYL4 OE, and PYL4^{A194T} OE plants (Fig. 7, A and B). However, we found that during the subsequent 5-d period, plant growth was reduced in nontransformed Col-0 and PYL4 OE plants compared with PYL4^{A194T} OE plants (Fig. 7B). Severe wilting and yellowing of leaves were observed at 16 d in the wild type, in contrast to PYL4^{A194T} OE lines. Finally, at 19 d, watering was resumed and survival of the plants was scored at 23 d. Col-0 wild-type plants did not survive after drought stress, whereas around 30% and 60% to 70% of PYL4 and PYL4^{A194T} OE lines survived, respectively (Fig. 7C). Finally, because PYL4^{A194T} OE lines were hypersensitive to ABA and showed derepression of ABA/drought-responsive genes, we tested whether they showed enhanced survival after suffering severe dehydration in petri dishes. These experiments were done using 15-d-old seedlings by submitting them to dehydration for 12 h in a laminar flow hood, followed by rehydration and scoring survival rate 3 d afterward. Dehydration experiments revealed enhanced resistance of PYL4^{A194T} OE compared with PYL4 OE and nontransformed plants. Thus, approximately 40% of PYL4^{A194T} plants survived after 12 h of dehydration followed by rehydration (Fig. 7D).

DISCUSSION

Under nonstress conditions, endogenous ABA levels play a critical role to regulate stomatal aperture, as

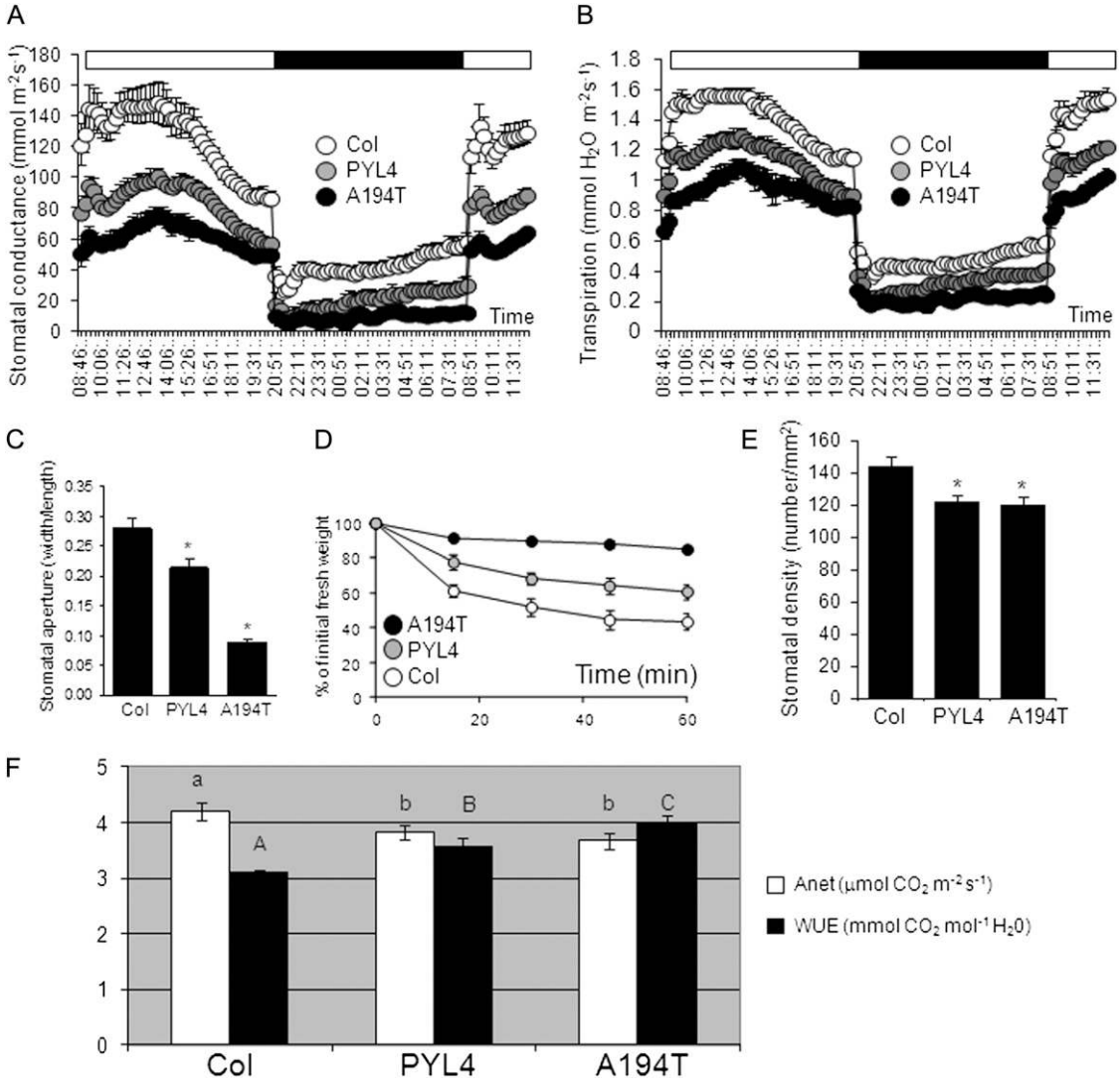

Figure 6. Leaf gas exchange measurements reveal reduced Gst and enhanced WUE in PYL4^{A194T} OE plants compared with nontransformed Col-0 and PYL4 OE plants. A and B, Gst and transpiration values of nontransformed Col-0, PYL4, and PYL4^{A194T} OE plants. Plants were kept in custom-made whole-rosette gas exchange measurement device (Kollist et al., 2007), and Gst and transpiration were followed during a diurnal light/dark cycle for 27 h. Values are mean ± SE ($n = 5$). White and black bars above represent light and dark periods, respectively. C, Reduced stomatal aperture of both PYL4 and PYL4^{A194T} OE lines compared with nontransformed Col-0 plants. Asterisk indicates $P < 0.05$ (Student's t test) when comparing data of OE lines and nontransformed Col-0 plants in the same assay conditions. D, Loss of fresh weight of 15-d-old plants submitted to the drying atmosphere of a laminar flow hood. E, Stomatal density is reduced in PYL4 and PYL4^{A194T} OE lines compared with nontransformed Col-0 plants. F, WUE is enhanced in PYL4^{A194T} OE lines compared with PYL4 OE and nontransformed plants. The values of Anet and WUE are averages for the whole day/light period. The different letters denote significant differences ($P < 0.05$; $n = 5$; ANOVA and Fisher's LSD test).

revealed by the open stomata phenotype of multiple *pyr/pyl* mutants, and basal ABA signaling is also required for proper plant growth and root development (Barrero et al., 2005; Gonzalez-Guzman et al., 2012; Antoni et al., 2013; Merilo et al., 2013). On the other hand, plant response to drought is largely dependent on enhanced ABA biosynthesis and signaling to regulate both stomatal aperture and gene expression under water stress conditions (Cutler et al., 2010). Thus, some mutants or transgenic plants showing enhanced response to ABA also display enhanced drought resistance and reduced water consumption (Pei et al., 1998; Hugouvieux et al., 2001; Saez et al., 2006). In this work, we describe a novel approach to confer drought resistance through genetic engineering of a mutated PYL4 receptor. The PYL4^{A194T} mutation here described cannot be considered a CA receptor, because we did not observe strong inhibition of PP2C activity in the absence of ABA. Triple and quadruple combinations of mutations were required to obtain CA PYR1, PYL2, and

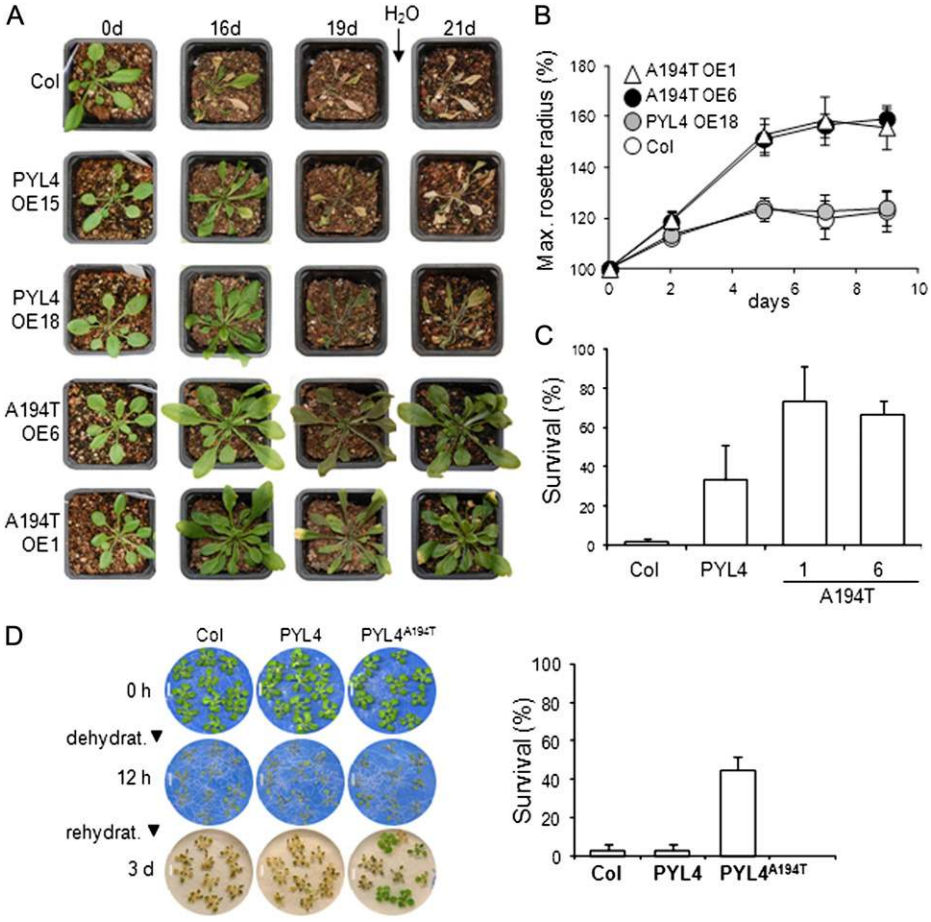

Figure 7. PYL4^{A194T} OE plants show enhanced drought and dehydration resistance. A, Enhanced drought resistance of PYL4^{A194T} OE plants with respect to nontransformed Col-0 or PYL4 OE plants. Two-week-old plants were deprived of water for 19 d and then rewatered. Photographs were taken at the start of the experiment (0 d), after 16 and 19 d of drought (16 and 19 d), and 2 d after rewatering (21 d from 0 d). Shoot was cut to better show the effect of drought on rosette leaves. B, Quantification of shoot growth (maximum rosette radius) of nontransformed Col-0, PYL4, and PYL4^{A194T} OE plants during the course of the experiment. Measurements were taken at different times (2, 5, 7, and 9 d) after the start of the experiment, and values at 0 d were taken as 100%. Values are means ± SE (n = 10). C, Survival percentage of nontransformed Col-0, PYL4, and PYL4^{A194T} OE plants 3 d after rewatering. Values are means ± SE from three independent experiments (n = 10 each). D, PYL4^{A194T} OE plants show enhanced resistance to dehydration. Two-week-old plants grown on MS plates were dehydrated by opening the lid in a laminar flow hood for 12 h (25°C ± 1°C and 25% ± 2% relative humidity) and next rehydrated, and survival was scored 3 d later. [See online article for color version of this figure.]

PYL9 receptors, which showed full ABA-independent inhibition of HAB1, ABI1, and ABI2 (Mosquna et al., 2011). As a result, expression of a 35S:GFP-PYL2^{CA} transgene in Arabidopsis seeds activated ABA signaling even in the ABA-deficient *aba2-1* mutant (Mosquna et al., 2011). However, the existence of a posttranscriptional mechanism that abolished expression of PYL2^{CA} in vegetative tissue precluded further analysis and testing of drought resistance in adult plants (Mosquna et al., 2011). The PYL4^{A194T} mutation improved ABA-dependent inhibition of PP2CA, and expression of the receptor could be detected in vegetative tissues of 35S:PYL4^{A194T} transgenic plants, which showed ABA hypersensitivity both in seed and vegetative responses. Moreover, 35S:PYL4^{A194T} exhibited enhanced drought resistance compared with nontransformed or 35S:PYL4 OE plants. Particularly interesting features were the partial derepression of ABA-responsive genes, reduced stomatal aperture, and transpiration of these lines at basal endogenous ABA levels. Additionally, because PYL4^{A194T} showed enhanced capacity to inhibit PP2CA at low ABA levels, it is likely that 35S:PYL4^{A194T} plants are primed for an accelerated response to stress conditions, which likely contributes to the enhanced drought resistance observed in these plants.

Y2H, in vitro protein-protein interaction, and BiFC assays revealed that PYL4^{A194T} showed a distinct pattern of interaction with PP2CA with respect to PYL4 (Figs. 1 and 3). Thus, both Y2H and pull-down assays indicated that PYL4^{A194T} interacted with PP2CA in the absence of ABA. BiFC assays showed enhanced interaction of PYL4^{A194T} and PP2CA compared with PYL4

at the endogenous ABA levels present in agroinfiltrated tobacco cells. ABA-independent interaction in Y2H assay does not necessarily imply capacity to inhibit phosphatase activity in the absence of ABA (Fujii et al., 2009; Ma et al., 2009; Park et al., 2009; Santiago et al., 2009b). In the absence of ABA, we only found a modest inhibitory effect of PYL4^{A194T} on PP2CA activity using pNPP but no significant effect when phosphorylated proteins were used as phosphatase substrate. By contrast, these substrates were better protected from PP2CA-mediated dephosphorylation by PYL4^{A194T} compared with PYL4 when ABA was present. It is likely that PYL4^{A194T} displays enhanced association kinetics with PP2CA than PYL4, particularly at low-intermediate levels of ABA, leading to enhanced formation of ternary complexes. Thus, PYL4^{A194T} might act at endogenous ABA levels or prime ABA-dependent interaction with PP2CA to speed initial response to stress. Additionally, the PYL4^{A194T}-PP2CA interaction might lead to steric hindrance of phosphatase activity in vivo by restricting access to the substrates. Steric inhibition of kinase activity by catalytically inactive phosphatase is well known in the field of ABA signaling (Lee et al., 2009; Soon et al., 2012). Thus, it was reported that an inactive form of PP2CA was able to inhibit SnRK2.6 kinase activity (Lee et al., 2009) and catalytically inactive HAB1 was still able to inhibit SnRK2.6 (Soon et al., 2012).

The effect of PYL4^{A194T} appeared to be specific for PP2CA with respect to HAB1, because it did not show a differential effect on HAB1 compared with PYL4. However, at this stage, we cannot exclude that other clade A phosphatases (for instance, other members of the PP2CA branch) might also be differentially affected by PYL4^{A194T}. Alignment of clade A PP2Cs reveals two subgroups (the ABI1 and PP2CA branches) and subtle differences in some regions of the proteins that could affect the interaction with PYR/PYLs (Bhaskara et al., 2012; Santiago et al., 2012). For instance, Bhaskara et al. (2012) noticed that HAI PP2Cs showed a differential interaction with PYR/PYLs and marked preference for monomeric receptors. Previous results revealed a certain specificity in the multiple interactions of the nine clade A PP2Cs and 14 PYR/PYLs (Santiago et al., 2009b; Szostkiewicz et al., 2010), and a differential inhibition of PP2CA by PYR/PYLs was recently reported (Antoni et al., 2012). Structural evidence for the PYL4^{A194T}-PP2CA complex is currently not available; however, taking as a model other complexes can be observed a clear difference in the length of the $\alpha 2\beta 4$ loop of clade A PP2Cs, which is close to the receptor-phosphatase binding interface (Fig. 8, A

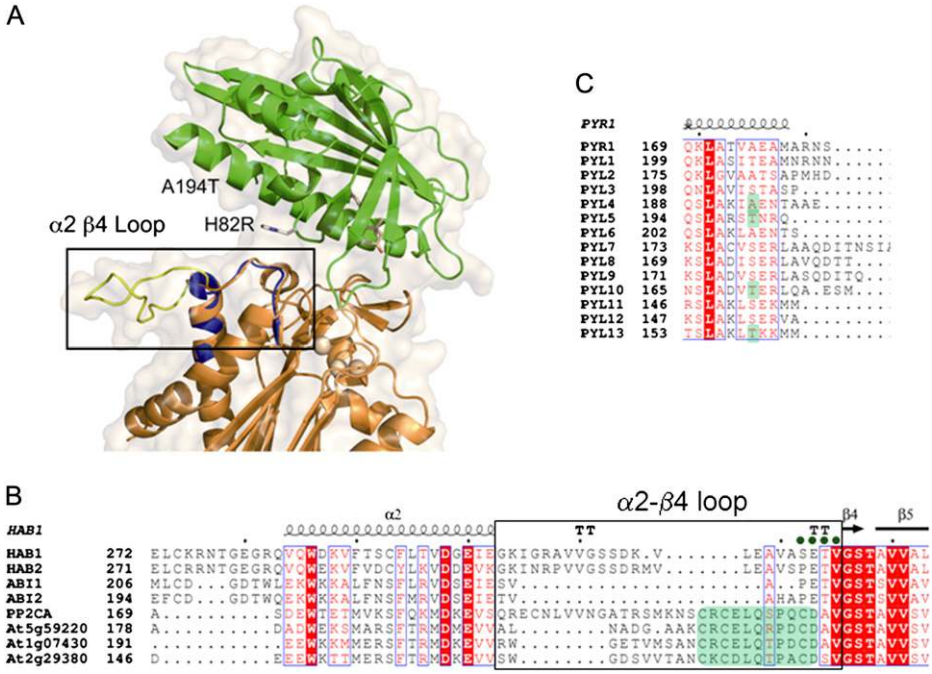

Figure 8. Modeling of PYL4^{A194T} and PYL4^{H82R} mutations based on the PYR1-ABA-HAB1 structure. A, Location on PYR1 of equivalent PYL4 A194T and H82R residues using structure of the PYR1 (green)-ABA-HAB1 (orange) complex (protein data bank code 3QN1). The variable $\alpha 2$-$\beta 4$ loop of clade A PP2Cs is displayed as a yellow ribbon for HAB1. The equivalent $\alpha 2$-$\beta 4$ loop from ABI1 (as deduced from the PYL1-ABA-ABI1 complex, protein data bank code 3KDJ) is displayed as a blue ribbon. B, The length of the $\alpha 2\beta 4$ loop (black box) notably differs among clade A PP2Cs. PP2CA displays the longer $\alpha 2\beta 4$ loop, and residues of the loop that show high identity with HAI PP2Cs (HAI1, At5g59220; HAI2, At1g07430; and HAI3, At2g29380) are highlighted in green. Amino acid residues of HAB1/ABI1 involved in the interaction with PYR/PYL receptors are marked as green dots. C, The location of the PYL4 A194 residue at the C-terminal α-helix and equivalent Thr residue of monomeric receptors PYL5, PYL10, and PYL13 is highlighted. [See online article for color version of this figure.]

and C). This $\alpha 2\beta 4$ loop is clearly different in PP2CA/HAI PP2Cs compared with the ABI1 branch, and it represents a potential point of interaction with PYL4^{A194T}. Additionally, the A194 residue is located at the C-terminal helix of PYL4, close to the receptor-phosphatase binding interface. Therefore, the A194T mutation might also indirectly influence the interaction of the C-terminal helix of PYL4 with PP2CA or establish new contact points with the $\alpha 2\beta 4$ loop of certain clade A PP2Cs. Interestingly, PYL10, which shows ABA-independent inhibition of PP2CA (Hao et al., 2011), contains a Thr residue at the equivalent position of PYL4^{A194T} (Fig. 8B).

In summary, genetic engineering of ABA receptors might serve as a new tool to ameliorate drought stress through (1) CA receptors (Mosquna et al., 2011), (2) mutations that enhance ABA-dependent inhibition of PP2Cs (this work), or (3) natural receptor versions that enhance ABA-independent inhibition of PP2Cs (Hao et al., 2011). Expression driven by a strong constitutive promoter might lead to some pleiotropic effects that negatively affect growth or yield of crop plants. Such a drawback could be bypassed by introducing stress-inducible or tissue-specific promoters that would drive the expression of the receptor only under stress conditions or in certain tissues.

MATERIALS AND METHODS

Plant Material and Growth Conditions

Arabidopsis (*Arabidopsis thaliana*) plants were routinely grown under greenhouse conditions (40%–50% relative humidity) in pots containing a vermiculite: soil (1:3) mixture. For plants grown under growth chamber conditions, seeds were surface sterilized by treatment with 70% (v/v) ethanol for 20 min, followed by commercial bleach (2.5% [v/v] sodium hypochlorite) containing 0.05% (v/v) Triton X-100 for 10 min and, finally, four washes with sterile distilled water. Stratification of the seeds was conducted in the dark at 4°C for 3 d. Seeds were sowed on MS plates composed of MS basal salts, 0.1% (v/v) MES, 1% (v/v) Suc, and 1% (w/v) agar. The pH was adjusted to 5.7 with KOH before autoclaving. Plates were sealed and incubated in a controlled environment growth chamber at 22°C under a 16-h-light/8-h-dark photoperiod at 80 to 100 μE m^{-2} sec^{-1}.

Construction of a PYL4 Mutant Library and Analysis of Y2H Interaction with PP2CA

We conducted error-prone PCR mutagenesis by amplification of the PYL4 open reading frame using the primers FPYL4NcoI, 5′-GCAGCAGCCATGGTTGCCG-TTCACCGTCCTTCT and RPYL4EcoRIstop, CGCACGAATTCACAGAGACA-TCTTCTTCTT and the following conditions: 2 mM dGTP, dCTP, and dTTP, 0.5 mM dATP, 12 mM $MgCl_2$, and Taq polymerase. The PCR product was *Nco*I-*Eco*RI doubly digested and cloned into the pGBKT7 vector, and DH10B cells were transformed by electroporation. Thus, we generated an allele library in *Escherichia coli* of approximately 10,000 PYL4 mutant clones. The sequencing of 50 clones revealed, on average, 1.7 nonsilent mutations per clone in the PYL4 sequence (207 amino acids). The library was shuttled to yeast (*Saccharomyces cerevisiae*) AH109 by cotransformation with pGAD7-PP2CA. Yeast transformants were pooled, and clones able to grow in the absence of exogenous ABA in medium lacking His and adenine were selected. Yeast plasmids were extracted, sequenced, and retransformed in yeast cells to recapitulate the phenotype. Protocols for Y2H assays were similar to those described previously (Saez et al., 2008).

BiFC Assay in *Nicotiana benthamiana*

Experiments were performed basically as described by Voinnet et al. (2003). The different binary vectors described above were introduced into *Agrobacterium tumefaciens* C58C1 (pGV2260; Deblaere et al., 1985) by electroporation, and transformed cells were selected in Luria-Bertani (LB) plates supplemented with kanamycin (50 μg mL^{-1}). Then they were grown in liquid LB medium to late exponential phase, and cells were harvested by centrifugation and resuspended in 10 mM morpholinoethanesulphonic acid-KOH (pH 5.6) containing 10 mM $MgCl_2$ and 150 mM acetosyringone to an optical density at 600 nm of 1. These cells were mixed with an equal volume of *A. tumefaciens* C58C1 (pCH32 35S:p19) expressing the silencing suppressor p19 of tomato bushy stunt virus (Voinnet et al., 2003) so that the final density of *A. tumefaciens* solution was about 1. Bacteria were incubated for 3 h at room temperature and then injected into young fully expanded leaves of 4-week-old *N. benthamiana* plants. Leaves were examined after 3 to 4 d under a Leica TCS-SL confocal microscope and laser scanning confocal imaging system. Quantification of fluorescent protein signal was done as described (Gampala et al., 2007) using the National Institutes of Health (NIH) Image software ImageJ v1.37.

Constructs were done in pSPYNE-35S (Walter et al., 2004) as well as gateway vector pYFP^{C}43 (a derivative of pMDC43 where GFP is replaced by YFP^{C}; Belda-Palazón et al., 2012). The coding sequence of At2g38310 (PYL4) was cloned into the pENTR223.1-Sfi entry vector, kindly provided by the Arabidopsis Biological Resource Center (clone G12806). The coding sequence of PYL4^{A194T} was PCR amplified, cloned into the pCR8/GW/TOPO, and verified by sequencing. Next, constructs containing PYL4 and PYL4^{A194T} were recombined by LR reaction into pYFP^{C}43 destination vector or into pH7WGR2 to generate RFP fusion proteins. The coding sequence of HAB1 and PP2CA was excised from a pCR8/GW/TOPO construct using a double digestion *Bam*HI-*Stu*I and subcloned into *Bam*HI-*Sma*I doubly digested pSPYNE-35S.

Protein Expression and Purification

For small-scale protein purifications, *E. coli* BL21 (DE3) cells transformed with the corresponding constructs were grown in 100 mL of LB medium to an optical density at 600 nm of 0.6 to 0.8. At this point, 1 mM isopropyl-β-D-thiogalactoside was added, and the cells were harvested after overnight incubation at 20°C. Pellets were resuspended in lysis buffer (50 mM Tris, pH 7.5, 250 mM KCl, 10% (v/v) glycerol, and 1 mM β-mercaptoethanol) and lysed by sonication with a Branson Sonifier 250. The clear lysate obtained after centrifugation was purified by Ni affinity. A washing step was performed using 50 mM Tris, 250 mM KCl, 20% (v/v) glycerol, 30 mM imidazole, and 1 mM β-mercaptoethanol washing buffer, and finally the protein was eluted using 50 mM Tris, 250 mM KCl, 20% (v/v) glycerol, 250 mM imidazole, and 1 mM β-mercaptoethanol elution buffer.

For protein-protein interaction experiments, the pET28a_ΔNPP2CA, pETM11_PYL4wt, and pETM11_PYL4^{A194T} plasmids were transformed into *E. coli* BL21 (DE3). A total of 8 mL of an overnight culture were subcultured into 800 mL fresh 2TY broth (16 g bacto-tryptone, 10 g yeast extract, and 5 g NaCl per liter of solution) plus kanamycin (50 μg ml^{-1}). Protein expression was induced with 0.3 mM isopropyl-β-D-thiogalactoside, and the cells were harvested after overnight incubation at 20°C. Pellets were resuspended in 25 mM Tris-HCl, pH 8.0, 50 mM NaCl, 50 mM imidazole, and 5 mM β-mercaptoethanol and disrupted by sonication. After centrifugation (40 min, 40,000*g*) at 277 K, the clear supernatant was filtered (pore diameter, 0.45 mm; Millipore Corporation). The 6His-tagged proteins were purified using nickel-nitrilotriacetic acid agarose (Qiagen) according to the manufacturer's instructions. The filtered supernatant was mixed with the previously equilibrated beads. After incubation, a washing step with 10 volumes of 25 mM Tris-HCl, pH 8.0, 50 mM NaCl, 20 mM imidazole, and 5 mM β-mercaptoethanol buffer was performed, followed by the elution from the Ni^{2+} resin in a buffer with 500 mM imidazole. Imidazole was removed using a PD-10 column (GE Healthcare), and the His tag was cleaved using tobacco etch virus protease.

Binding Assay of 6His-ΔNPP2CA and PYL4

6His-ΔNPP2CA pellets were resuspended in 25 mM Tris-HCl, pH 8.0, 150 mM NaCl, 50 mM imidazole, 5 mM β-mercaptoethanol, and 5 mM Mg^{2+}, mixed with 8 mg of either pure nontagged (through tobacco etch virus cleavage) PYL4 or PYL4^{A194T}, and disrupted by sonication. The crude extracts were treated as described above using His-Trap HP columns from GE Healthcare to the capture step according to the manufacturer's instructions. In all cases, the purified proteins were subjected to a size exclusion chromatography using a Superdex200 10/300 (Amersham Biosciences Limited) to analyze the behavior in a gel filtration of each protein and to isolate the complex. To perform pull-down assays, 6His-ΔNPP2CA was purified, next immobilized on nickel-nitrilotriacetic acid agarose beads (Qiagen), and incubated with either pure nontagged PYL4 or PYL4^{A194T}. The mix was swirled 30 min at 4°C and incubated in the absence or presence of

100 μM ABA. After three washes, proteins were eluted by adding 500 mM imidazol and analyzed by SDS-PAGE.

PP2C and OST1 in Vitro Activity Assays

Phosphatase activity was measured using as a substrate either pNPP or phosphorylated ΔC-ABF2, ΔC-ABI5, and SLAC1$^{1–186}$ proteins. For the pNPP substrate, assays were performed in a 100-μL solution containing 25 mM Tris-HCl, pH 7.5, 2 mM $MnCl_2$, and 5mM pNPP. Assays contained 2 μM phosphatase (PP2CA or HAB1), 4 μM receptor, and the indicated concentrations of ABA. Phosphatase activity was recorded with a ViktorX5 reader at 405 nm every 60 s over 30 min, and the activity obtained after 30 min is indicated in the graphics. To obtain phosphorylated ΔC-ABF2, ΔC-ABI5, and SLAC1$^{1–186}$ proteins, phosphorylation reactions were done using the OST1 kinase basically as described previously (Dupeux et al., 2011b). ΔC-ABF2 and SLAC1$^{1–186}$ N-terminal fragments were prepared as described (Vahisalu et al., 2010; Antoni et al., 2012). ΔC-ABI5 recombinant protein (amino acid residues 1–200, containing the C1, C2, and C3 target sites of ABA-activated SnRK2s) was expressed in the pETM11 vector as described above. The reaction mixture containing the OST1 kinase and either ΔC-ABF2, ΔC-ABI5, or SLAC1$^{1–186}$ recombinant proteins was incubated for 50 min at room temperature in 30 μL of kinase buffer: 20 mM Tris-HCl, pH 7.8, 20 mM $MgCl_2$, 2 mM $MnCl_2$, and 3.5 μCi of γ-^{32}ATP (3,000 Ci mmol^{-1}). Thus, OST1 was autophosphorylated, and in turn, it phosphorylated ΔC-ABF2, ΔC-ABI5, and SLAC1$^{1–186}$ proteins. Next, they were used as substrates of PP2CA that was preincubated (or not) for 10 min with PYL4 or PYL4^{A194T} either in the absence or presence of the indicated ABA concentration. The reaction was stopped by adding Laemmli buffer, and the proteins were separated by SDS-PAGE using an 8% (v/v) acrylamide gel and transferred to an Immobilon-P membrane (Millipore). Radioactivity was detected and quantified using a Phosphorimage system (FLA5100, Fujifilm). After scanning, the same membrane was used for Ponceau staining. The data presented are averages of at least three independent experiments.

Generation of Transgenic Lines

PYL4 or PYL4 mutants were cloned into pCR8/GW/TOPO entry vector (Invitrogen) and recombined by LR reaction into the Gateway-compatible ALLIGATOR2 vector (Bensmihen et al., 2004). This construct drives expression of PYL4 under control of the *Cauliflower mosaic virus* 35S promoter and introduces a triple HA epitope at the N terminus of the protein. Selection of transgenic lines is based on the visualization of GFP in seeds, whose expression is driven by the specific seed promoter At2S3. The ALLIGATOR2-35S:3HA-PYL4 or mutant constructs were transferred to *A. tumefaciens* C58C1 (pGV2260; Deblaere et al., 1985) by electroporation and used to transform Col-0 wild-type plants by the floral dip method. T1 transgenic seeds were selected based on GFP visualization and sowed in soil to obtain the T2 generation. At least three independent transgenic lines were generated for each construct. Homozygous T3 progeny was used for further studies, and expression of HA-tagged protein in 21-d-old seedlings was verified by immunoblot analysis using anti-HA-peroxidase (Roche).

Seed Germination and Seedling Establishment Assays

After surface sterilization of the seeds, stratification was conducted in the dark at 4°C for 3 d. Approximately 100 seeds of each genotype were sowed on MS plates supplemented with different ABA concentrations per experiment. To score seed germination, radical emergence was analyzed at 72 h after sowing. Seedling establishment was scored as the percentage of seeds that developed green expanded cotyledons and the first pair of true leaves.

Root and Shoot Growth Assays

Seedlings were grown on vertically oriented MS plates for 4 to 5 d. Afterward, 20 plants were transferred to new MS plates lacking or supplemented with the indicated concentrations of ABA. The plates were scanned on a flatbed scanner after 10 d to produce image files suitable for quantitative analysis of root growth using the NIH software ImageJ v1.37. As an indicator of shoot growth, the maximum rosette radius was measured.

RNA Analyses

ABA treatment, RNA extraction, and quantitative reverse transcription-PCR amplifications were performed as previously described (Saez et al., 2004).

Whole-Rosette Stomatal Conductance and Transpiration Measurements

The Arabidopsis whole-rosette gas exchange measurement device, plant growth practice, and custom written program to calculate transpiration and Gst for water vapor have been described previously (Kollist et al., 2007; Vahisalu et al., 2008). For gas exchange experiments, 25- to 28-d-old plants (rosette area, 6–18 cm^2) were used. Until measurements, plants were grown in growth chambers (AR-66LX and AR-22L, Percival Scientific) at 12/12 photoperiod, 23°C/18°C temperature, air relative humidity of 70% to 75% and 150 μmol m^{-2} s^{-1} light. During gas exchange measurements, temperature, air relatively humidity, photoperiod, and light in the cuvettes were kept as similar as possible to the values in growth chambers. Photographs of plants were taken before and after the experiment, and rosette leaf area was calculated using the NIH software ImageJ 1.37v. Leaf area values for the intermediary experimental period were calculated using linear regression between starting and final leaf area.

Water Loss and Stomatal Aperture Assays

Two- to three-week-old seedlings grown in MS plates were used for water loss assays. Four seedlings per genotype with similar growth (three independent experiments) were submitted to the drying atmosphere of a laminar flow hood. Kinetic analysis of water loss was performed and represented as the percentage of initial fresh weight loss at each scored time point. Stomatal aperture measurements were done in leaves of 5-week-old plants grown under greenhouse conditions using whole-leaf imaging (Chitrakar and Melotto, 2010). Staining of whole leaves with propidium iodide was conducted, and the aperture of 30 to 40 stomata (ratio, width/length; two independent experiments) was measured using a Leica TCS-SL confocal microscope.

Drought Stress

Plants grown under greenhouse conditions (10 individuals per experiment, three independent experiments) were grown under normal watering conditions for 15 d and then subjected to drought stress by stopping irrigation during 20 d. Next, watering was resumed, and survival rate was calculated after 3 d by counting the percentage of plants that had more than four green leaves. Photographs were taken at the start of the experiment (day 0), after 16 and 19 d of drought, and 3 d after rewatering. Quantification of shoot growth was performed at 2, 5, 7 and 9 d after stopping irrigation (day 0) by measuring the maximum rosette radius of the plants.

Dehydration Treatment

Two-week-old seedlings grown in MS plates were used for these experiments. Twenty seedlings per genotype (two independent experiments) were submitted to the drying atmosphere of a laminar flow hood for 12 h (25°C ± 1°C, 25% ± 2% relative humidity) and then rehydrated with 25 mL of water. Survival percentage was scored 3 d after rehydration by counting the percentage of plants that had at least four green leaves.

The Arabidopsis Genome Initiative locus identifiers for *PYL4* and *PP2CA* are *At2g38310* and *At3g11410*, respectively.

Supplemental Data

The following materials are available in the online version of this article.

Supplemental Figure S1. ABA infiltration reveals BiFC interaction of PYL4 and PP2CA, both at nucleus and cytosol.

Supplemental Figure S2. Enhanced sensitivity to ABA-mediated inhibition of germination and early seedling growth in T4 PYL4^{A194T} OE plants compared with nontransformed Col-0 and PYL4 OE plants.

Received July 2, 2013; accepted July 17, 2013; published July 17, 2013.

LITERATURE CITED

Antoni R, Gonzalez-Guzman M, Rodriguez L, Rodrigues A, Pizzio GA, Rodriguez PL (2012) Selective inhibition of clade A phosphatases type 2C by PYR/PYL/RCAR abscisic acid receptors. Plant Physiol **158:** 970–980

Antoni R, Gonzalez-Guzman M, Rodriguez L, Peirats-Llobet M, Pizzio GA, Fernandez MA, De Winne N, De Jaeger G, Dietrich D, Bennett MJ, et al (2013) PYRABACTIN RESISTANCE1-LIKE8 plays an important role for the regulation of abscisic acid signaling in root. Plant Physiol **161:** 931–941

Barrero JM, Piqueras P, González-Guzmán M, Serrano R, Rodríguez PL, Ponce MR, Micol JL (2005) A mutational analysis of the ABA1 gene of *Arabidopsis thaliana* highlights the involvement of ABA in vegetative development. J Exp Bot **56:** 2071–2083

Belda-Palazón B, Ruiz L, Martí E, Tárraga S, Tiburcio AF, Culiáñez F, Farràs R, Carrasco P, Ferrando A (2012) Aminopropyltransferases involved in polyamine biosynthesis localize preferentially in the nucleus of plant cells. PLoS ONE **7:** e46907

Bensmihen S, To A, Lambert G, Kroj T, Giraudat J, Parcy F (2004) Analysis of an activated ABI5 allele using a new selection method for transgenic Arabidopsis seeds. FEBS Lett **561:** 127–131

Bhaskara GB, Nguyen TT, Verslues PE (2012) Unique drought resistance functions of the highly ABA-induced clade A protein phosphatase 2Cs. Plant Physiol **160:** 379–395

Chitrakar R, Melotto M (2010) Assessing stomatal response to live bacterial cells using whole leaf imaging. J Vis Exp **44:** e2185

Cutler SR, Rodriguez PL, Finkelstein RR, Abrams SR (2010) Abscisic acid: emergence of a core signaling network. Annu Rev Plant Biol **61:** 651–679

Deblaere R, Bytebier B, De Greve H, Deboeck F, Schell J, Van Montagu M, Leemans J (1985) Efficient octopine Ti plasmid-derived vectors for *Agrobacterium*-mediated gene transfer to plants. Nucleic Acids Res **13:** 4777–4788

Dupeux F, Antoni R, Betz K, Santiago J, Gonzalez-Guzman M, Rodriguez L, Rubio S, Park SY, Cutler SR, Rodriguez PL, et al (2011b) Modulation of abscisic acid signaling in vivo by an engineered receptor-insensitive protein phosphatase type 2C allele. Plant Physiol **156:** 106–116

Dupeux F, Santiago J, Betz K, Twycross J, Park SY, Rodriguez L, Gonzalez-Guzman M, Jensen MR, Krasnogor N, Blackledge M, et al (2011a) A thermodynamic switch modulates abscisic acid receptor sensitivity. EMBO J **30:** 4171–4184

Fujii H, Chinnusamy V, Rodrigues A, Rubio S, Antoni R, Park SY, Cutler SR, Sheen J, Rodriguez PL, Zhu JK (2009) In vitro reconstitution of an abscisic acid signalling pathway. Nature **462:** 660–664

Gampala SS, Kim TW, He JX, Tang W, Deng Z, Bai MY, Guan S, Lalonde S, Sun Y, Gendron JM, et al (2007) An essential role for 14-3-3 proteins in brassinosteroid signal transduction in Arabidopsis. Dev Cell **13:** 177–189

Gonzalez-Guzman M, Pizzio GA, Antoni R, Vera-Sirera F, Merilo E, Bassel GW, Fernández MA, Holdsworth MJ, Perez-Amador MA, Kollist H, et al (2012) *Arabidopsis* PYR/PYL/RCAR receptors play a major role in quantitative regulation of stomatal aperture and transcriptional response to abscisic acid. Plant Cell **24:** 2483–2496

Hao Q, Yin P, Li W, Wang L, Yan C, Lin Z, Wu JZ, Wang J, Yan SF, Yan N (2011) The molecular basis of ABA-independent inhibition of PP2Cs by a subclass of PYL proteins. Mol Cell **42:** 662–672

Hugouvieux V, Kwak JM, Schroeder JI (2001) An mRNA cap binding protein, ABH1, modulates early abscisic acid signal transduction in Arabidopsis. Cell **106:** 477–487

Iuchi S, Kobayashi M, Taji T, Naramoto M, Seki M, Kato T, Tabata S, Kakubari Y, Yamaguchi-Shinozaki K, Shinozaki K (2001) Regulation of drought tolerance by gene manipulation of 9-cis-epoxycarotenoid dioxygenase, a key enzyme in abscisic acid biosynthesis in Arabidopsis. Plant J **27:** 325–333

Jakab G, Ton J, Flors V, Zimmerli L, Métraux JP, Mauch-Mani B (2005) Enhancing Arabidopsis salt and drought stress tolerance by chemical priming for its abscisic acid responses. Plant Physiol **139:** 267–274

Kollist T, Moldau H, Rasulov B, Oja V, Ramma H, Huve K, Jaspers P, Kangasjarvi J, Kollist H (2007) A novel device detects a rapid ozone-induce transient stomatal closure in intact Arabidopsis and its absence in abi2 mutant. Physiol Plant **129:** 796–803

Kuhn JM, Boisson-Dernier A, Dizon MB, Maktabi MH, Schroeder JI (2006) The protein phosphatase *AtPP2CA* negatively regulates abscisic acid signal transduction in Arabidopsis, and effects of *abh1* on *AtPP2CA* mRNA. Plant Physiol **140:** 127–139

Lackman P, González-Guzmán M, Tilleman S, Carqueijeiro I, Pérez AC, Moses T, Seo M, Kanno Y, Häkkinen ST, Van Montagu MC, et al (2011) Jasmonate signaling involves the abscisic acid receptor PYL4 to regulate metabolic reprogramming in Arabidopsis and tobacco. Proc Natl Acad Sci USA **108:** 5891–5896

Lee SC, Lan W, Buchanan BB, Luan S (2009) A protein kinase-phosphatase pair interacts with an ion channel to regulate ABA signaling in plant guard cells. Proc Natl Acad Sci USA **106:** 21419–21424

Ma Y, Szostkiewicz I, Korte A, Moes D, Yang Y, Christmann A, Grill E (2009) Regulators of PP2C phosphatase activity function as abscisic acid sensors. Science **324:** 1064–1068

Merilo E, Laanemets K, Hu H, Xue S, Jakobson L, Tulva I, Gonzalez-Guzman M, Rodriguez PL, Schroeder JI, Broschè M, et al (2013) PYR/RCAR receptors contribute to ozone-, reduced air humidity-, darkness-, and CO_2-induced stomatal regulation. Plant Physiol **162:** 1652–1668

Mosquna A, Peterson FC, Park SY, Lozano-Juste J, Volkman BF, Cutler SR (2011) Potent and selective activation of abscisic acid receptors in vivo by mutational stabilization of their agonist-bound conformation. Proc Natl Acad Sci USA **108:** 20838–20843

Park SY, Fung P, Nishimura N, Jensen DR, Fujii H, Zhao Y, Lumba S, Santiago J, Rodrigues A, Chow TFF, et al (2009) Abscisic acid inhibits type 2C protein phosphatases via the PYR/PYL family of START proteins. Science **324:** 1068–1071

Pei ZM, Ghassemian M, Kwak CM, McCourt P, Schroeder JI (1998) Role of farnesyltransferase in ABA regulation of guard cell anion channels and plant water loss. Science **282:** 287–290

Qin X, Zeevaart JA (2002) Overexpression of a 9-cis-epoxycarotenoid dioxygenase gene in *Nicotiana plumbaginifolia* increases abscisic acid and phaseic acid levels and enhances drought tolerance. Plant Physiol **128:** 544–551

Saavedra X, Modrego A, Rodríguez D, González-García MP, Sanz L, Nicolás G, Lorenzo O (2010) The nuclear interactor PYL8/RCAR3 of *Fagus sylvatica* FsPP2C1 is a positive regulator of abscisic acid signaling in seeds and stress. Plant Physiol **152:** 133–150

Saez A, Apostolova N, Gonzalez-Guzman M, Gonzalez-Garcia MP, Nicolas C, Lorenzo O, Rodriguez PL (2004) Gain-of-function and loss-of-function phenotypes of the protein phosphatase 2C HAB1 reveal its role as a negative regulator of abscisic acid signalling. Plant J **37:** 354–369

Saez A, Robert N, Maktabi MH, Schroeder JI, Serrano R, Rodriguez PL (2006) Enhancement of abscisic acid sensitivity and reduction of water consumption in Arabidopsis by combined inactivation of the protein phosphatases type 2C ABI1 and HAB1. Plant Physiol **141:** 1389–1399

Saez A, Rodrigues A, Santiago J, Rubio S, Rodriguez PL (2008) HAB1-SWI3B interaction reveals a link between abscisic acid signaling and putative SWI/SNF chromatin-remodeling complexes in *Arabidopsis*. Plant Cell **20:** 2972–2988

Santiago J, Dupeux F, Betz K, Antoni R, Gonzalez-Guzman M, Rodriguez L, Márquez JA, Rodriguez PL (2012) Structural insights into PYR/PYL/RCAR ABA receptors and PP2Cs. Plant Sci **182:** 3–11

Santiago J, Dupeux F, Round A, Antoni R, Park SY, Jamin M, Cutler SR, Rodriguez PL, Márquez JA (2009a) The abscisic acid receptor PYR1 in complex with abscisic acid. Nature **462:** 665–668

Santiago J, Rodrigues A, Saez A, Rubio S, Antoni R, Dupeux F, Park SY, Márquez JA, Cutler SR, Rodriguez PL (2009b) Modulation of drought resistance by the abscisic acid receptor PYL5 through inhibition of clade A PP2Cs. Plant J **60:** 575–588

Soon FF, Ng LM, Zhou XE, West GM, Kovach A, Tan MH, Suino-Powell KM, He Y, Xu Y, Chalmers MJ, et al (2012) Molecular mimicry regulates ABA signaling by SnRK2 kinases and PP2C phosphatases. Science **335:** 85–88

Szostkiewicz I, Richter K, Kepka M, Demmel S, Ma Y, Korte A, Assaad FF, Christmann A, Grill E (2010) Closely related receptor complexes differ in their ABA selectivity and sensitivity. Plant J **61:** 25–35

Tallman G (2004) Are diurnal patterns of stomatal movement the result of alternating metabolism of endogenous guard cell ABA and accumulation of ABA delivered to the apoplast around guard cells by transpiration? J Exp Bot **55:** 1963–1976

Vahisalu T, Kollist H, Wang YF, Nishimura N, Chan WY, Valerio G, Lamminmäki A, Brosché M, Moldau H, Desikan R, et al (2008) SLAC1 is required for plant guard cell S-type anion channel function in stomatal signalling. Nature **452:** 487–491

Vahisalu T, Puzõrjova I, Brosché M, Valk E, Lepiku M, Moldau H, Pechter P, Wang YS, Lindgren O, Salojärvi J, et al (2010) Ozone-triggered rapid stomatal response involves the production of reactive oxygen species, and is controlled by SLAC1 and OST1. Plant J **62:** 442–453

Voinnet O, Rivas S, Mestre P, Baulcombe D (2003) An enhanced transient expression system in plants based on suppression of gene silencing by the p19 protein of tomato bushy stunt virus. Plant J **33:** 949–956

Walter M, Chaban C, Schütze K, Batistic O, Weckermann K, Näke C, Blazevic D, Grefen C, Schumacher K, Oecking C, et al (2004) Visualization of protein interactions in living plant cells using bimolecular fluorescence complementation. Plant J **40:** 428–438

Yoshida T, Nishimura N, Kitahata N, Kuromori T, Ito T, Asami T, Shinozaki K, Hirayama T (2006) ABA-hypersensitive germination3 encodes a protein phosphatase 2C (AtPP2CA) that strongly regulates abscisic acid signaling during germination among Arabidopsis protein phosphatase 2Cs. Plant Physiol **140:** 115–126

Zhang X, Zhang Q, Xin Q, Yu L, Wang Z, Wu W, Jiang L, Wang G, Tian W, Deng Z, et al (2012) Complex structures of the abscisic acid receptor PYL3/RCAR13 reveal a unique regulatory mechanism. Structure **20:** 780–790